

# Statistical Broadband over Power Lines Channel Modeling — Part 1: The Theory of the Statistical Hybrid Model

Athanasios G. Lazaropoulos\*

**Abstract**—This pair of papers proposes a new approach towards the channel modeling of transmission and distribution broadband over power lines (BPL) networks either on the theoretical or on the practical basis. The proposed statistical hybrid model is the synthesis of the well-validated deterministic hybrid model and a set of well-known statistical distributions widely used in communications literature such as Gaussian, Lognormal, Wald, Weibull and Gumbel statistical distributions. In this paper, the theoretical framework of the statistical hybrid model, as well as the flowchart of the statistical hybrid model, is analytically presented.

## 1. INTRODUCTION

Transmission and distribution power grids represent an omnipresent widely branched hierarchical structure that facilitates the power delivery from producers to consumers. During recent years, the glaring transformation of the traditional power grid to the smart grid also allows the development of a parallel advanced IP-based communications network enhanced with a plethora of broadband applications [1–13]. Hence, the integration of the communications network information is one of the key issues in the design of the smart grid. Among the available communications solutions, Broadband over Power Lines (BPL) technology can play an important role since it exploits the already installed wired power grid infrastructure [14–22].

Considered as a transmission medium for communications signals, transmission and distribution power grids are subjected to various inherent deficiencies such as high and frequency-selective channel attenuation [18–21, 23–27]. As the modeling of BPL channel attenuation is concerned, until now, BPL channel models basically follow either a bottom-up approach or a top-down approach or appropriate syntheses of the aforementioned approaches [3, 15, 18–22, 28–43]. Among the available state-of-art BPL channel models in the literature, the deterministic hybrid model, which is denoted simply as hybrid model, has been extensively employed to examine the behavior of various multiconductor transmission line (MTL) configurations in transmission and distribution BPL networks [4, 18–22, 28, 31, 33, 34, 38]. Through its two interconnected modules, namely: (i) the bottom-up approach module that is based on an appropriate combination of MTL theory and similarity transformations and (ii) the top-down approach module that is based on the concatenation of multidimensional transmission matrices of the cascaded network BPL connections, the hybrid model gives as output crucial broadband performance metrics of the examined BPL networks such as channel attenuation and capacity.

In this paper, the hybrid model is adopted as the reference BPL channel model and further statistically extended. Although statistical evaluation of transmission and distribution BPL networks has provided interesting results in [22, 28] concerning their channel attenuation and capacity behavior, the definition of a statistical BPL channel modeling remains an interesting challenge. So far, a number

---

*Received 29 January 2019, Accepted 28 March 2019, Scheduled 5 April 2019*

\* Corresponding author: Athanasios G. Lazaropoulos (AGLazaropoulos@gmail.com).

The author is with the School of Electrical and Computer Engineering, National Technical University of Athens, 9, Iroon Polytechniou Street, GR 15780, Zografou Campus, Athens, Greece.

of scientific efforts have focused on the proposal of statistical BPL channel models that exploit either the bottom-up approach or the top-down approach and their corresponding measurement data, simulation results, and numerical findings [28, 44–50]. In this paper, the proposed statistical hybrid model is based on the formality and validity of the deterministic hybrid model while its results are considered as the filtered hybrid model results through a set of proper channel attenuation statistical distributions, which are well known in the communications research fields, such as Gaussian, Lognormal, Wald, Weibull, and Gumbel channel attenuation distributions [51]. The results of the proposed statistical hybrid model provide capacity ranges for given injected power spectral density (IPSD) limit, noise PSD level, coupling scheme, and BPL topology class where a BPL topology class consists of overhead Medium-Voltage (OV MV) and underground Medium-Voltage (UN MV) BPL topologies that come from the channel attenuation statistical distribution processing of the respective indicative BPL topologies. In fact, the exact theoretical procedure of implementing a statistical hybrid model, which comprises the reception and processing of the input data of the hybrid model, the definition of the applied channel attenuation distributions, the computation of the maximum likelihood estimators (MLEs) of the channel attenuation statistical distributions, the definition of the random number generator based on the respective channel attenuation distribution MLEs, and the computation of the capacity ranges of distribution BPL topology classes, is detailed in this paper. In the companion paper of [52], the numerical results concerning the statistical hybrid model are demonstrated.

The rest of this paper is organized as follows. In Section 2, OV MV and UN MV MTL configurations and indicative distribution BPL topologies, which are adopted in this paper, are presented. Section 3 summarizes the basics of the hybrid model and coupling schemes. In Section 4, a small briefing regarding the IPSD limits, noise PSD levels, and capacity computations is given. Section 5 synthesizes the knowledge of Sections 6–7 towards the definition of the proposed statistical hybrid model. Section 6 concludes this paper.

## 2. DISTRIBUTION MTL CONFIGURATIONS AND BPL TOPOLOGIES

In this Section, a brief synopsis of the OV MV and UN MV MTL configurations used in this paper is demonstrated as well as the required topological characteristics of the applied indicative OV MV and UN MV BPL topologies.

### 2.1. OV MV and UN MV MTL Configurations

A typical case of OV MV distribution line is depicted in Fig. 1(a). This OV MV distribution line consists of three parallel non-insulated phase conductors ( $n^{\text{OV MV}} = 3$ ) spaced by  $\Delta^{\text{OV MV}}$  and hangs at typical heights  $h^{\text{OV MV}}$  above lossy ground. This three-phase three-conductor MTL configuration consists of

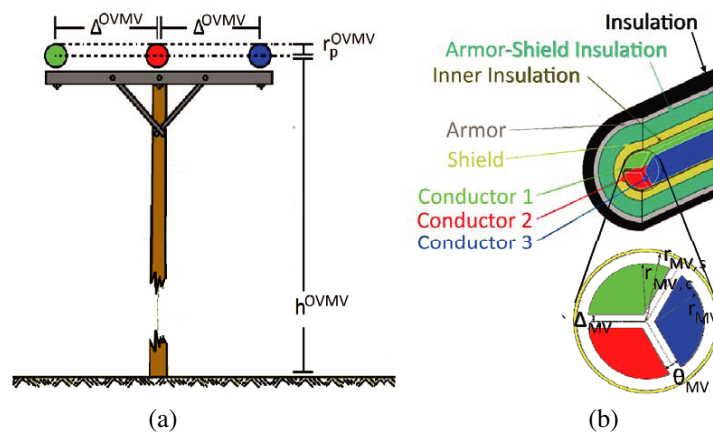


**Figure 1.** Typical distribution MTL configurations [28]. (a) OV MV. (b) UN MV.

Aluminium-Conductor Steel-Reinforced (ACSR) conductors while the exact dimensions of this OV MV MTL configuration are given in [28].

A typical case of UN MV distribution line is depicted in Fig. 1(b). In fact, this UN MV distribution line is the three-phase sector-type paper insulated lead covered (PILC) distribution-class cable (8/10 kV,  $3 \times 95 \text{ mm}^2 \text{ Cu}$ ). The cable arrangement consists of the three-phase three-sector-type conductors, one shield conductor, and one armor conductor. The shield and armor are grounded at both ends [20, 28, 53–55]. Due to the common UN practice of grounding at both ends, the analysis in this UN MV MTL configuration is focused only on the inner conductor set of the three phases and the shield ( $n^{\text{UNMV}} = 3$ ). The exact dimensions of this UN MV MTL configuration are given in [28].

During the propagation analysis of OV MV and UN MV MTL configurations, a lossy ground is considered as the reference conductor. Its conductivity is assumed  $\sigma_g = 5 \text{ mS/m}$ , and its relative permittivity  $\epsilon_{rg} = 13$ . In accordance with [3, 18, 19, 22, 31, 56–60], the aforementioned ground properties can define a realistic scenario suitable for the impact analysis of imperfect ground on BPL signal propagation via OV MV MTL configurations. As already mentioned, the impact of imperfect ground on BPL signal propagation via UN MV MTL configurations remains negligible.

### 2.2. Indicative OV MV and UN MV BPL Topologies

BPL networks exploit the already existing infrastructure of power grids and its surrounding environment by deploying BPL equipment units (such as BPL extractors and injectors), smart meters, sensors, and other pieces of smart grid equipment that collect, receive, and transmit information in the context of BPL signals. In accordance with [6, 14, 20, 28] and with reference to Fig. 2, BPL networks can be divided into cascaded BPL connections, which can be treated separately as cascaded network modules. Each BPL connection that is denoted as BPL topology is bounded by the transmitting end and receiving end repeaters while different numbers of branches  $k$ ,  $k = 1, \dots, N$ , distribution cable lengths  $L_k$ ,  $k = 1, \dots, N + 1$ , and branch lengths  $L_{bk}$ ,  $k = 1, \dots, N$  are encountered across the BPL signal transmission path. In Fig. 2, a typical BPL topology, which is handled by the hybrid model, is shown where the aforementioned topological characteristics are reported.

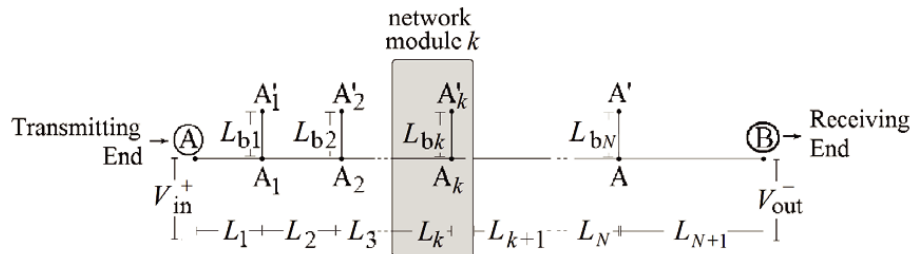


**Figure 2.** Typical BPL topology with  $N$  branches [28].

With reference to Fig. 2, five indicative OV MV and UN MV BPL topologies are reported in Tables 1 and 2, respectively. With reference to [19, 21, 26, 28], the indicative OV MV and UN MV BPL topologies concern average long end-to-end connections of 1000 m and 200 m, respectively, while these indicative OV MV and UN MV topologies act as the BPL topology class representatives and are reported in Tables 1 and 2, respectively. Anyway, the statistical processing of the statistical hybrid model is based on the channel attenuation results of these indicative OV MV and UN MV BPL topologies.

As the circuital parameters of the above indicative OV MV and UN MV BPL topologies are concerned, these are detailed in [3, 14–16, 18–22, 28, 31, 33, 38, 53, 56, 61–70]. Synoptically, the required assumptions concerning these circuital parameters can be reported as follows: (i) the branching cables are assumed identical to the distribution cables; (ii) the interconnections between the distribution and branch conductors are fully activated; say all the phase and neutral conductors of the branching cables are connected to the respective ones of the distribution cables; (iii) the transmitting and receiving ends are assumed to be matched to the characteristic impedance of the modal channels; and (iv) the branch terminations are assumed open circuit.

**Table 1.** Indicative OV MV BPL topologies [5].

Topology Number ( $l$ )	Topology Name	BPL Topology Class Description	Member Number in the BPL Topology Class ( $p$ )	Number of Branches	Length of Distribution Lines	Length of Branching Lines
1	Urban case A	Typical OV MV BPL urban topology class	1	3	$L_1 = 500$ m, $L_2 = 200$ m, $L_3 = 100$ m, $L_4 = 200$ m	$L_{b1} = 8$ m, $L_{b2} = 13$ m, $L_{b3} = 10$ m
2	Urban case B	Aggravated OV MV BPL urban topology class	1	5	$L_1 = 200$ m, $L_2 = 50$ m, $L_3 = 100$ m, $L_4 = 200$ m, $L_5 = 300$ m, $L_6 = 150$ m	$L_{b1} = 12$ m, $L_{b2} = 5$ m, $L_{b3} = 28$ m, $L_{b4} = 41$ m, $L_{b5} = 17$ m
3	Suburban case	OV MV BPL suburban topology class	1	2	$L_1 = 500$ m, $L_2 = 400$ m, $L_3 = 100$ m	$L_{b1} = 50$ m, $L_{b2} = 10$ m
4	Rural case	OV MV BPL rural topology class	1	1	$L_1 = 600$ m, $L_2 = 400$ m	$L_{b1} = 300$ m
5	“LOS” case	OV MV BPL Line-of-Sight transmission class	1	0	$L_1 = 1000$ m	-

**Table 2.** Indicative UN MV BPL topologies [5].

Topology Number ( $l$ )	Topology Name	BPL Topology Class Description	Member Number in the BPL Topology Class ( $p$ )	Number of Branches	Length of Distribution Lines	Length of Branching Lines
1	Urban case A	Typical UN MV BPL urban topology class	1	3	$L_1 = 70$ m, $L_2 = 55$ m, $L_3 = 45$ m, $L_4 = 30$ m	$L_{b1} = 12$ m, $L_{b2} = 7$ m, $L_{b3} = 21$ m
2	Urban case B	Aggravated UN MV BPL urban topology class	1	5	$L_1 = 40$ m, $L_2 = 10$ m, $L_3 = 20$ m, $L_4 = 40$ m, $L_5 = 60$ m, $L_6 = 30$ m	$L_{b1} = 22$ m, $L_{b2} = 12$ m, $L_{b3} = 8$ m, $L_{b4} = 2$ m, $L_{b5} = 17$ m
3	Suburban case	UN MV BPL suburban topology class	1	2	$L_1 = 50$ m, $L_2 = 100$ m, $L_3 = 50$ m	$L_{b1} = 60$ m, $L_{b2} = 30$ m
4	Rural case	UN MV BPL rural topology class	1	1	$L_1 = 50$ m, $L_2 = 150$ m	$L_{b1} = 100$ m
5	“LOS” case	UN MV BPL “LOS” transmission class	1	0	$L_1 = 200$ m	-

### 3. HYBRID MODEL AND COUPLING SCHEMES

Since more than two conductors are encountered in OV MV and UN MV MTL configurations, the standard TL analysis should be extended to the MTL case [3, 15, 18–22, 28, 32]. In this Section, the hybrid model, which describes the BPL propagation and transmission, is briefly presented while the coupling schemes, which adjust the way that the BPL signal power is injected into and extracted from the cables, are also outlined. Note that both the hybrid model and coupling schemes are demonstrated in terms of their channel attenuation findings that are going to be further exploited by the statistical hybrid model.

#### 3.1. Hybrid Model

On the basis of its two interconnected modules, say, the bottom-up and top-down approach modules, several useful performance metrics such as channel attenuation and capacity may be calculated by the hybrid model. Extensively analyzed in [3, 14, 15, 18–22, 28, 32, 40, 41], OV MV and UN MV MTL configurations with  $n^G$  phase conductors may support  $n^G$  modes that propagate across MTL BPL configurations where  $[\cdot]^G$  denotes the examined distribution power grid type (i.e., OV MV or UN MV). Through Transmission Matrix version 2 (TM2) method, which is based on the scattering matrix formalism and is part of the top-down approach of the hybrid model, the  $n^G \times n^G$  channel transfer function matrix  $\mathbf{H}^G \{\cdot\}$  that relates line quantities with modal ones is determined from

$$\mathbf{H}^G \{\cdot\} = \mathbf{T}_V^G \cdot \mathbf{H}^{G,m} \{\cdot\} \cdot (\mathbf{T}_V^G)^{-1} \quad (1)$$

where  $\mathbf{H}^{G,m} \{\cdot\}$  is the  $n^G \times n^G$  modal channel transfer function matrix of the examined distribution power grid type that mainly depends on the examined distribution BPL topology, and  $\mathbf{T}_V^G$  is a  $n^G \times n^G$  matrix that depends on the frequency, examined distribution power grid type, physical properties of the cables, and geometry of the MTL configuration.

#### 3.2. CS2 Module and Coupling Schemes

According to how signals are injected into and extracted from the lines of OV MV and UN MV BPL networks, different coupling schemes may exist, which are implemented by coupling scheme modules (CS modules) integrated in the top-down approach of the hybrid model [3, 5, 28, 31, 71]. With reference to [5, 71], CS2 module, which is the most recently upgraded coupling scheme module for BPL networks, can describe the BPL signal coupling procedure by using two interfaces, namely: (i) BPL signal injection interface — see Fig. 3(a) — and (ii) BPL signal extraction interface — see Fig. 3(b) —. In terms of transfer function and with reference to Eq. (1), CS2 module computes the coupling scheme channel transfer function that relates output BPL signal  $V^{\text{out-}}$  and input BPL signal  $V^{\text{in+}}$  through

$$H^{G,C} \{\cdot\} = [\mathbf{C}^{\text{out}}]^{G,C} \cdot \mathbf{H}^G \{\cdot\} \cdot [\mathbf{C}^{\text{in}}]^{G,C} \quad (2)$$

where  $\mathbf{C}^{\text{in}}$  is the input coupling  $n^G \times 1$  column vector that deals with the BPL signal injection interface and consists of the input coupling coefficients  $C_i^{\text{in}}$ ,  $i = 1, \dots, n^G$ ;  $\mathbf{C}^{\text{out}}$  is the output coupling  $1 \times n^G$  line vector that deals with the BPL signal extraction interface and consists of the output coupling coefficients  $C_i^{\text{out}}$ ,  $i = 1, \dots, n^G$ ; and  $[\cdot]^C$  denotes the applied coupling scheme. On the basis of Eq. (2) and depending on the form of  $\mathbf{C}^{\text{in}}$  and  $\mathbf{C}^{\text{out}}$ , CS2 module can support three types of coupling schemes, namely: (1) *Coupling Scheme Type 1: Wire-to-Ground (WtG) or Shield-to-Phase (StP)* coupling schemes for OV or UN BPL networks, respectively; (2) *Coupling Scheme Type 2: Wire-to-Wire (WtW) or Phase-to-Phase (PtP)* coupling schemes for OV or UN BPL networks, respectively; and (3) *Coupling Scheme Type 3: MultiWire-to-MultiWire (MtM) or MultiPhase-to-MultiPhase (MtM)* coupling schemes for OV or UN BPL networks, respectively. Depending on the involved conductors of the examined MTL configuration and the power restrictions of [5, 71], concerning the definition of  $\mathbf{C}^{\text{in}}$  and  $\mathbf{C}^{\text{out}}$ , different coupling schemes can occur for given coupling scheme type. As presented in Section 5, all the required statistical processing of the statistical hybrid model is made on the basis of the coupling scheme channel transfer function of Eq. (2).

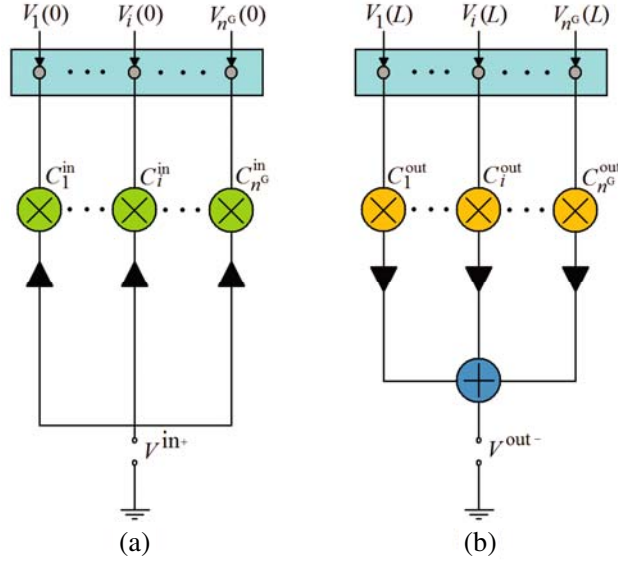


**Figure 3.** CS2 module [71]. (a) BPL signal injection interface at the transmitting end. (b) BPL signal extraction interface at the receiving end.

#### 4. IPSD LIMITS, NOISE AND CAPACITY OF DISTRIBUTION BPL TOPOLOGIES

Capacity is defined as the maximum achievable transmission rate that can be reliably transmitted over a BPL topology. Apart from the coupling scheme channel transfer function of Section 3, IPSD limits and noise PSD levels are defined in this Section for the OV MV and UN MV BPL networks so that the capacity of a BPL topology can be computed.

##### 4.1. IPSD Limits

The frequency range that is used by BPL systems to operate is common with other already licensed communications services. Hence, BPL systems are, at the same time, transmitters of unintentionally electromagnetic interference (EMI) to these already licensed communications services (e.g., aeronautical radionavigation, radio astronomy, mobile satellite and maritime mobile), and receivers of EMI from the aforementioned services. In order to regulate EMI from BPL systems, a great number of regulatory bodies have established proposals (EMI policies) as well as respective IPSD limits concerning the BPL operation. By adopting these EMI policies, the emissions from BPL networks are regulated so as not to interfere with the other already existing communications services in the same frequency band of operation. Among the proposals concerning EMI policies, the most noted are FCC Part 15, German Reg TP NB30, and the BBC/NATO Proposal. The electric field strength limits proposed by the above proposals are presented in [24, 72, 73]. From these limits, the respective IPSD limits are determined in [73] for OV MV and UN MV BPL networks.

##### 4.2. Noise PSD Levels

As already mentioned in [3, 14–16, 18–22, 28], OV MV and UN MV BPL networks suffer from colored background and impulsive noise, which are the dominant noise types in BPL networks. In accordance with [74], noise has been identified as a leading inherent BPL deficiency that may severely degrade the BPL capacity performance. However, FL noise model, which is the abbreviated name of the spectrally flat additive white Gaussian (AWGN) noise, has been proven in [74] to be an efficient and precise tool for computing the capacities of distribution BPL networks in the 3–30 MHz frequency ranges. Hence, as the noise properties of OV MV and UN MV BPL networks are concerned in the 3–30 MHz frequency range, AWGN PSD levels will be assumed equal to  $-60$  dBm/Hz and  $-40$  dBm/Hz in the case of OV MV and UN MV BPL networks, respectively.

### 4.3. Capacity

As already defined in the introduction of this Section, capacity depends on the applied MTL configuration, examined distribution BPL topology, applied coupling scheme, adopted EMI policies, and noise environment [3, 14–20]. The capacity  $C$  for given coupling scheme channel is given by

$$C = f_s \sum_{q=1}^Q \log_2 \left\{ 1 + \left[ \frac{\langle p(f_q) \rangle_L}{\langle N(f_q) \rangle_L} \cdot |H^{G,C}(f_q)|^2 \right] \right\} \quad (3)$$

where

$$f_q = 3 \text{ MHz} + (q - 1) \cdot f_s, \quad q = 1, \dots, Q \quad (4)$$

is the flat-fading subchannel start frequency,  $f_s$  the flat-fading subchannel frequency spacing,  $Q$  the number of subchannels in the examined 3–30 MHz frequency range,  $p(\cdot)$  the applied IPSD limits in dBm/Hz,  $N(\cdot)$  the applied AWGN PSD levels IPSD noise level in dBm/Hz, and  $\langle \cdot \rangle_L$  an operator that converts dBm/Hz into a linear power ratio (W/Hz).

With reference to Eq. (3), the main output of the statistical hybrid method, which is numerically presented in [75], is the capacity range of a BPL topology class when different channel attenuation statistical distributions are going to be applied as described in Section 5.

## 5. FLOWCHART OF THE STATISTICAL HYBRID MODEL

Until now, Sections 2–4 focused on the brief presentation of the hybrid model that is, anyway, the core element of the statistical hybrid model. In order to transform the deterministic results of the hybrid model to the stochastic capacity range results of the statistical hybrid model, the description of the statistical hybrid model needs to be detailed in this Section.

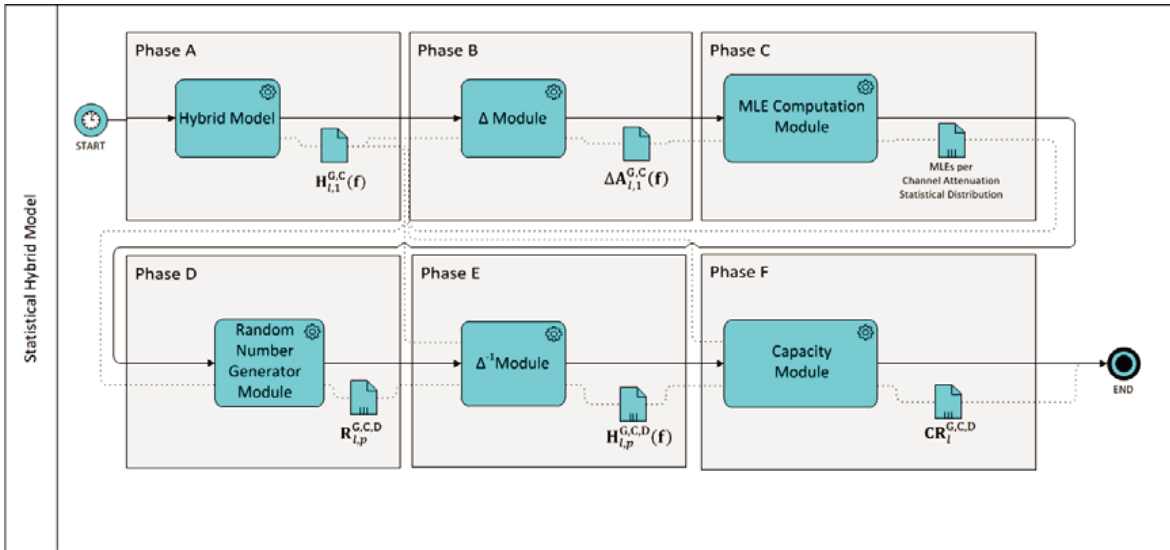


Figure 4. BPMN diagram of the statistical hybrid model.

In Fig. 4, a flowchart of the statistical hybrid model is expressed as a business process model notification (BPMN) diagram. From Fig. 4, it is evident that there are six phases (i.e., Phase A-F) so that the deterministic coupling scheme channel transfer function results of the hybrid model are converted into the stochastic capacity range results of the statistical hybrid model. More specifically:

- *Phase A:* With reference to Sections 2 and 3, hybrid model takes as inputs the distribution power grid type, the indicative distribution BPL topology of Tables 1 or 2 as well as the respective

distribution MTL configuration and the applied coupling scheme. The hybrid model gives as outputs the coupling scheme channel transfer function  $1 \times Q$  line vector  $\mathbf{H}_{l,p}^{G,C}(\mathbf{f})$  where  $\mathbf{f}$  is the  $1 \times Q$  line vector that consists of the flat-fading subchannel start frequencies  $f_q$ ,  $q = 1, \dots, Q$ ;  $l$  is the topology number (see Tables 1 and 2); and  $p$ ,  $p = 1, \dots, P + 1$ , is the member number in the BPL topology class (see Tables 1 and 2). Here, it should be noted that each indicative distribution BPL topology of Tables 1 and 2 is uniquely characterized by its distribution power grid type  $G$  and its topology number  $l$ . Also, each indicative distribution BPL topology of Tables 1 and 2 acts as the first member of its respective BPL topology class (i.e.,  $p = 1$ ) while the other  $[(P + 1) - 2 + 1] = P$  members of the class will be defined in Phase E (i.e.,  $p = 2, \dots, P + 1$ ).

- *Phase B:* Since coupling scheme channel transfer function is well delivered by Phase A, the coupling scheme channel attenuation difference module  $\Delta$  of this Phase is responsible for estimating the channel attenuation differences of the different indicative distribution BPL topologies with respect to the “LOS” case for given distribution power grid type and coupling scheme. In accordance with [4, 18, 22, 28], “LOS” case channel attenuation remains the lowest in the vast majority of the cases among the different BPL topologies for given distribution power grid type and coupling scheme. Hence, the coupling scheme channel attenuation difference between each indicative distribution BPL topology and its respective “LOS” case remains positive in all the examined flat-fading subchannels in the vast majority of the cases and is given by:

$$\Delta A_{l,1}^{G,C}(\mathbf{f}) = - \left[ \mathbf{H}_{l,1}^{G,C}(\mathbf{f}) - \mathbf{H}_{5,1}^{G,C}(\mathbf{f}) \right] \quad (5)$$

Note that for the “LOS” case, the coupling scheme channel attenuation difference is always equal to zero regardless of the distribution power grid type and the coupling scheme.

- *Phase C:* MLE computation method helps towards the MLE estimation of the applied channel attenuation statistical distributions given the coupling scheme channel attenuation differences of the Phase B. Since a set of channel attenuation statistical distributions is examined in this paper, each of them is characterized by its own set of MLEs for given coupling scheme channel attenuation difference. To schematically represent the existence of different MLE sets, three small vertical lines, which are anyway provided by the BPMN standard, have been applied to the output file of Phase C in the BPMN diagram of Fig. 4. Here, it should be noted that for the specific channel attenuation statistical distribution, MLEs can be found as an explicit function of the coupling scheme channel attenuation differences while for other statistical distributions, MLEs can only be determined via numerical optimization since no closed-form solution is available. As the channel attenuation statistical distributions are concerned, their MLE estimation method is presented in Appendix A.
- *Phase D:* The main component of this Phase is the random number generator module, which takes as input the MLEs of the applied channel attenuation statistical distributions of Phase C. Since MLEs of each channel attenuation statistical distribution are already known, so does cumulative density function (CDF) of each distribution (see Appendix A). In accordance with [76, 77], since CDFs of each channel attenuation statistical distribution can be easily determined, the random number  $1 \times Q$  line vector  $\mathbf{R}_{l,p}^{G,C,D}$  is produced by the random number generator module for given power grid type, coupling scheme, and indicative distribution BPL topology where  $[\cdot]^D$  denotes the channel attenuation statistical distribution that is adopted in order to generate random numbers (i.e., Gaussian, Lognormal, Wald, Weibull, and Gumbel distributions). Note that each power grid type, indicative distribution BPL topology, coupling scheme, and channel attenuation statistical distribution define  $P$  random number line vectors as the number of members of each BPL topology class, which will be defined in Phase E.
- *Phase E:* Phase E performs the inverse procedure of Phase B through its  $\Delta^{-1}$  module. By appropriately combining coupling scheme channel transfer function  $\mathbf{H}_{5,1}^{G,C}(\mathbf{f})$  of Phase A and random number line vectors  $\mathbf{R}_{l,p}^{G,C,D}$  of Phase D, the coupling scheme channel transfer function line vector of each of the  $P$  members of each BPL topology class is determined by:

$$\mathbf{H}_{l,p}^{G,C,D}(\mathbf{f}) = \mathbf{H}_{5,1}^{G,C}(\mathbf{f}) - \mathbf{R}_{l,p}^{G,C,D} \quad (6)$$

for given power grid type, coupling scheme, and channel attenuation statistical distribution. Now each OV MV and UN MV BPL topology class consists of  $P+1$  members whose coupling scheme channel transfer functions for given power grid type, coupling scheme, and channel attenuation statistical distribution are considered as the output of the Phase E.

- *Phase F.* Phase F receives the output of Phase E and further computes the capacity range of each BPL topology class for given power grid type, coupling scheme, and channel attenuation statistical distribution. With reference to Eq. (3), the capacity  $C_{l,p}^{G,C,D}$  of the respective coupling scheme channel transfer function line vector  $\mathbf{H}_{l,p}^{G,C,D}(\mathbf{f})$  can be computed. Distribution BPL topology class capacity  $\mathbf{C}_l^{G,C,D}$  consists of all the capacities of its  $P+1$  members, say

$$\mathbf{C}_l^{G,C,D} = \left[ C_{l,1}^{G,C,D} \quad \dots \quad C_{l,p}^{G,C,D} \quad \dots \quad C_{l,P+1}^{G,C,D} \right] \quad (7)$$

Therefore, the capacity range of each OV MV and UN MV BPL topology class  $l$ , which is the output of the Phase F and of the statistical hybrid model, is equal to

$$\mathbf{CR}_l^{G,C,D} = \left[ \min \left\{ \mathbf{C}_l^{G,C,D} \right\} \quad \text{avg} \left\{ \mathbf{C}_l^{G,C,D} \right\} \quad \max \left\{ \mathbf{C}_l^{G,C,D} \right\} \right] \quad (8)$$

where  $\min \{ \cdot \}$ ,  $\text{avg} \{ \cdot \}$  and  $\max \{ \cdot \}$  computes the minimum, average, and maximum values for given power grid type, coupling scheme, and channel attenuation statistical distribution.

Synopsizing this Section, statistical hybrid model is based on the distribution “LOS” cases in order to enrich the existing distribution BPL topology classes of hybrid model, which initially consists of only one representative distribution BPL topology, with  $P$  members for given power grid type, coupling scheme, and channel attenuation statistical distribution. Since distribution BPL topology classes comprise  $P + 1$  distribution BPL topologies, statistical hybrid model computes the capacity ranges of each distribution BPL topology class for given power grid type, coupling scheme, and channel attenuation statistical distribution. Note that BPL topology classes of distribution “LOS” cases act as the distribution BPL topology base for the statistical hybrid model and, for that reason, practically consist of only one topology for given power grid type, coupling scheme, and channel attenuation statistical distribution; say, distribution “LOS” case.

Finally, it is obvious that power grid types, BPL topology classes, coupling schemes, and channel attenuation statistical distributions have different impacts on capacity ranges of the statistical hybrid model. In order to investigate and assess the behavior of the statistical hybrid model, simulated and numerical results are presented in the companion paper of [52]. In [52], the Gaussian, Lognormal, Wald, Weibull, and Gumbel channel attenuation statistical distributions are going to be benchmarked for various power grid types, IPSD limits, noise PSD levels, and coupling schemes in terms of the capacity estimation success. The success of MLE and capacity estimations is going to be associated and examined by applying the proposed metrics of the capacity percentage change and the average absolute capacity percentage change.

## 6. CONCLUSIONS

In this paper, the theoretical framework and flowchart of the statistical hybrid model have been proposed. More analytically, the statistical hybrid model consists of 6 phases while the well-verified hybrid model acts as the core element of the statistical hybrid model. The channel attenuation statistical distributions of this paper, say, Gaussian, Lognormal, Wald, Weibull, and Gumbel distributions, receive as input the coupling scheme channel attenuation results of the hybrid model. Apart from the MLE estimation, channel attenuation statistical distributions cooperate with the random number generator so that the enrichment of BPL topology classes can occur with BPL topology members of same MLEs with the representative indicative BPL topology per each examined channel attenuation statistical distribution.

The output of the statistical hybrid model is the capacity range of each OV MV and UN MV BPL topology class for given power grid type, IPSD limit, noise PSD level, coupling scheme, and channel attenuation statistical distribution. The numerical results of the statistical hybrid model are presented in [52].

## APPENDIX A.

In this pair of papers, five well-known statistical distributions widely used in communications literature such as Gaussian, Lognormal, Wald, Weibull and Gumbel distributions are assumed. Among the other critical parameters of the statistical hybrid model described in Section 5, the involvement of channel attenuation statistical distributions in the statistical hybrid model is concentrated on the Phases C and D of the statistical hybrid model as presented in Fig. 4. More analytically:

- As Phase C is concerned, MLE computation module estimates the MLEs of each applied channel attenuation statistical distribution by receiving the data of coupling scheme channel attenuation difference  $\Delta \mathbf{A} = [ \Delta A_1 \ \cdots \ \Delta A_q \ \cdots \ \Delta A_Q ]$  from Phase B as determined in Eq. (5). Note that the coupling scheme channel attenuation difference has been selected so that its results remain always positive.
- As Phase D is concerned, the random number generator module gives as output random number line vectors by exploiting the CDFs of each applied channel attenuation statistical distribution as detailed in [76, 77]. Since MLEs of each applied channel attenuation statistical distribution are already known from Phase C, the respective CDF can be numerically estimated.

Therefore, the CDF and MLEs of each applied channel attenuation statistical distribution with respect to the data of coupling scheme channel attenuation difference are here given.

### A.1. Gaussian Channel Attenuation Distribution

The Gaussian distribution, also known as the normal distribution, is often used in sciences to represent random variables whose distributions are not known. Its CDF is given by

$$\text{CDF}^{\text{Gaussian}}(\Delta A_q) = \frac{1}{2} \cdot \left[ 1 + \text{erf} \left( \frac{\Delta A_q - \hat{\mu}_{\text{MLE}}^{\text{Gaussian}}}{\hat{\sigma}_{\text{MLE}}^{\text{Gaussian}} \cdot \sqrt{2}} \right) \right] \quad (\text{A1})$$

where

$$\hat{\mu}_{\text{MLE}}^{\text{Gaussian}} = \Delta \bar{A}_q \equiv \frac{1}{Q} \cdot \sum_{q=1}^Q (\Delta A_q) \quad (\text{A2})$$

$$(\hat{\sigma}_{\text{MLE}}^{\text{Gaussian}})^2 = \frac{1}{Q} \cdot \sum_{q=1}^Q (\Delta A_q - \Delta \bar{A}_q)^2 \quad (\text{A3})$$

Note that  $\hat{\mu}_{\text{MLE}}^{\text{Gaussian}}$  and  $\hat{\sigma}_{\text{MLE}}^{\text{Gaussian}}$  are the MLEs of the Gaussian channel attenuation distribution and are computed by a closed form solution.

### A.2. Lognormal Channel Attenuation Distribution

The form of a lognormal channel attenuation distribution CDF is given by

$$\text{CDF}^{\text{Lognormal}}(\Delta A_q) = \frac{1}{2} + \frac{1}{2} \cdot \text{erf} \left[ \frac{\ln(\Delta A_q) - \hat{\mu}_{\text{MLE}}^{\text{Lognormal}}}{\sqrt{2} \cdot \hat{\sigma}_{\text{MLE}}^{\text{Lognormal}}} \right] \quad (\text{A4})$$

where

$$\hat{\mu}_{\text{MLE}}^{\text{Lognormal}} = \frac{\sum_{q=1}^Q [\ln(\Delta A_q)]}{Q} \quad (\text{A5})$$

$$\left( \hat{\sigma}_{\text{MLE}}^{\text{Lognormal}} \right)^2 = \frac{\sum_{q=1}^Q \left[ \ln(\Delta A_q) - \hat{\mu}_{\text{MLE}}^{\text{Lognormal}} \right]^2}{Q} \quad (\text{A6})$$

Note that  $\hat{\mu}_{\text{MLE}}^{\text{Lognormal}}$  and  $\hat{\sigma}_{\text{MLE}}^{\text{Lognormal}}$  are the MLEs of the Lognormal channel attenuation distribution and are computed by a closed form solution.

### A.3. Wald Channel Attenuation Distribution

With reference to [78], the Wald distribution, also known as the inverse Gaussian distribution, is a two-parameter continuous distribution whose CDF is given by

$$\text{CDF}^{\text{Wald}}(\Delta A_q) = \Phi \left[ \sqrt{\frac{\hat{\lambda}_{\text{MLE}}^{\text{Wald}}}{\Delta A_q}} \cdot \left( \frac{\Delta A_q}{\hat{\mu}_{\text{MLE}}^{\text{Wald}}} - 1 \right) \right] + \exp \left( \frac{2 \cdot \hat{\lambda}_{\text{MLE}}^{\text{Wald}}}{\hat{\mu}_{\text{MLE}}^{\text{Wald}}} \right) \cdot \Phi \left[ -\sqrt{\frac{\hat{\lambda}_{\text{MLE}}^{\text{Wald}}}{\Delta A_q}} \cdot \left( \frac{\Delta A_q}{\hat{\mu}_{\text{MLE}}^{\text{Wald}}} + 1 \right) \right], \Delta A_q \geq 0 \quad (\text{A7})$$

where

$$\hat{\mu}_{\text{MLE}}^{\text{Wald}} = \frac{\sum_{q=1}^Q (\Delta A_q)}{Q} \quad (\text{A8})$$

$$\hat{\lambda}_{\text{MLE}}^{\text{Wald}} = \frac{Q}{\sum_{q=1}^Q \left( \frac{1}{\Delta A_q} - \frac{1}{\hat{\mu}_{\text{MLE}}^{\text{Wald}}} \right)} \quad (\text{A9})$$

and  $\Phi \{ \cdot \}$  is the Gaussian CDF of Eq. (A1) with  $\hat{\mu}_{\text{MLE}}^{\text{Gaussian}}$  and  $\hat{\sigma}_{\text{MLE}}^{\text{Gaussian}}$  equal to 0 and 1, respectively.

Note that  $\hat{\mu}_{\text{MLE}}^{\text{Wald}}$  and  $\hat{\lambda}_{\text{MLE}}^{\text{Wald}}$  are the MLEs of the Wald channel attenuation distribution and are a closed form solution.

### A.4. Weibull Channel Attenuation Distribution

With reference to [79, 80], the form of a two-parameter Weibull channel attenuation distribution CDF is given by

$$\text{CDF}^{\text{Weibull}}(\Delta A_q) = \begin{cases} 1 - \exp \left[ - \left( \frac{\Delta A_q}{\hat{a}_{\text{MLE}}^{\text{Weibull}}} \right)^{\hat{\beta}_{\text{MLE}}^{\text{Weibull}}} \right], & \Delta A_q \geq 0 \\ 0, & \text{elsewhere} \end{cases} \quad (\text{A10})$$

where

$$\hat{a}_{\text{MLE}}^{\text{Weibull}} = \left\{ \frac{1}{Q} \cdot \sum_{q=1}^Q \left[ (\Delta A_q)^{\hat{\beta}_{\text{MLE}}^{\text{Weibull}}} \right] \right\}^{\frac{1}{\hat{\beta}_{\text{MLE}}^{\text{Weibull}}}} \quad (\text{A11})$$

$$\frac{1}{\hat{\beta}_{\text{MLE}}^{\text{Weibull}}} + \frac{1}{Q} \cdot \sum_{q=1}^Q [\ln(\Delta A_q)] - \frac{\sum_{q=1}^Q \left[ (\Delta A_q)^{\hat{\beta}_{\text{MLE}}^{\text{Weibull}}} \cdot \ln(\Delta A_q) \right]}{\sum_{q=1}^Q \left[ (\Delta A_q)^{\hat{\beta}_{\text{MLE}}^{\text{Weibull}}} \right]} = 0 \quad (\text{A12})$$

Note that  $\hat{a}_{\text{MLE}}^{\text{Weibull}}$  and  $\hat{\beta}_{\text{MLE}}^{\text{Weibull}}$  are the MLEs of the Weibull channel attenuation distribution and are not a closed form solution.  $\hat{\beta}_{\text{MLE}}^{\text{Weibull}}$  is obtained by using the Newton-Raphson in Eq. (A12) while  $\hat{a}_{\text{MLE}}^{\text{Weibull}}$  follows by substituting  $\hat{\beta}_{\text{MLE}}^{\text{Weibull}}$  in Eq. (A11).

### A.5. Gumbel Channel Attenuation Distribution

With reference to [81], the form of a two-parameter Gumbel channel attenuation distribution CDF is given by

$$\text{CDF}^{\text{Gumbel}}(\Delta A_q) = \exp \left\{ - \exp \left[ - \frac{(\Delta A_q - \hat{\epsilon}_{\text{MLE}}^{\text{Gumbel}})}{\hat{a}_{\text{MLE}}^{\text{Gumbel}}} \right] \right\} \quad (\text{A13})$$

where

$$\Delta \hat{A}_q = \hat{a}_{\text{MLE}}^{\text{Gumbel}} + \frac{\sum_{q=1}^Q \left[ \Delta A_q \cdot \exp \left( -\frac{\Delta A_q}{\hat{a}_{\text{MLE}}^{\text{Gumbel}}} \right) \right]}{\sum_{q=1}^Q \left[ \exp \left( -\frac{\Delta A_q}{\hat{a}_{\text{MLE}}^{\text{Gumbel}}} \right) \right]} \quad (\text{A14})$$

$$\hat{c}_{\text{MLE}}^{\text{Gumbel}} = \hat{a}_{\text{MLE}}^{\text{Gumbel}} \cdot \left\{ \ln(Q) - \ln \left[ \sum_{q=1}^Q \exp \left( -\frac{\Delta A_q}{\hat{a}_{\text{MLE}}^{\text{Gumbel}}} \right) \right] \right\} \quad (\text{A15})$$

Note that  $\hat{a}_{\text{MLE}}^{\text{Gumbel}}$  and  $\hat{c}_{\text{MLE}}^{\text{Gumbel}}$  are the MLEs of the Gumbel channel attenuation distribution and are not a closed form solution.  $\hat{a}_{\text{MLE}}^{\text{Gumbel}}$  is obtained by using the Newton-Raphson in Eq. (A14) and  $\hat{c}_{\text{MLE}}^{\text{Gumbel}}$  is then implicitly obtained from Eq. (A15) after the substitution of  $\hat{a}_{\text{MLE}}^{\text{Gumbel}}$ .

## REFERENCES

1. Lazaropoulos, A. G., “A panacea to inherent BPL technology deficiencies by deploying broadband over power lines (BPL) connections with multi-hop repeater systems,” *Bentham Recent Advances in Electrical & Electronic Engineering*, Vol. 10, No. 1, 30–46, 2017.
2. Aalamifar, F. and L. Lampe, “Optimized WiMAX profile configuration for smart grid communications,” *IEEE Transactions on Smart Grid*, Vol. 8, No. 6, 2723–2732, 2017.
3. Lazaropoulos, A. G., “Deployment concepts for overhead high voltage broadband over power lines connections with two-hop repeater system: Capacity countermeasures against aggravated topologies and high noise environments,” *Progress In Electromagnetics Research B*, Vol. 44, 283–307, 2012.
4. Lazaropoulos, A. G., “Towards broadband over power lines systems integration: Transmission characteristics of underground low-voltage distribution power lines,” *Progress In Electromagnetics Research B*, Vol. 39, 89–114, 2012.
5. Lazaropoulos, A. G., “Broadband performance metrics and regression approximations of the new coupling schemes for distribution broadband over power lines (BPL) networks,” *Trends in Renewable Energy*, Vol. 4, No. 1, 43–73, Jan. 2018, [Online]. Available: <http://futureenergysp.com/index.php/tre/article/view/59/pdf>.
6. Lazaropoulos, A. G., “Wireless sensor network design for transmission line monitoring, metering and controlling introducing broadband over powerlines-enhanced network model (BPLeNM),” *ISRN Power Engineering*, Vol. 2014, Article ID 894628, 22 pages, 2014, [Online]. Available: <http://www.hindawi.com/journals/isrn.power.engineering/2014/894628/>.
7. Lazaropoulos, A. G., “Improvement of power systems stability by applying topology identification methodology (TIM) and fault and instability identification methodology (FIIM) — Study of the overhead medium-voltage broadband over power lines (OV MV BPL) networks case,” *Trends in Renewable Energy*, Vol. 3, No. 2, 102–128, Apr. 2017. [Online]. Available: <http://futureenergysp.com/index.php/tre/article/view/34>
8. Lazaropoulos, A. G., “Main line fault localization methodology in smart grid — Part 1: Extended TM2 method for the overhead medium-voltage broadband over power lines networks case,” *Trends in Renewable Energy*, Vol. 3, No. 3, 2–25, Dec. 2017, [Online]. Available: <http://futureenergysp.com/index.php/tre/article/view/36>.
9. Lazaropoulos, A. G., “Main line fault localization methodology in smart grid — Part 2: Extended TM2 method, measurement differences and L1 piecewise monotonic data approximation for the overhead medium-voltage broadband over power lines networks case,” *Trends in Renewable Energy*, Vol. 3, No. 3, 26–61, Dec. 2017, [Online]. Available: <http://futureenergysp.com/index.php/tre/article/view/37>.

10. Lazaropoulos, A. G., "Main line fault localization methodology in smart grid — Part 3: Main line fault localization methodology (MLFLM)," *Trends in Renewable Energy*, Vol. 3, No. 3, 62-81, Dec. 2017, [Online]. Available: <http://futureenergysp.com/index.php/tre/article/view/38>.
11. Lazaropoulos, A. G., "Main line fault localization methodology (MLFLM) in smart grid — The underground medium- and low-voltage broadband over power lines networks case," *Trends in Renewable Energy*, Vol. 4, No. 1, 15-42, Dec. 2017, [Online]. Available: <http://futureenergysp.com/index.php/tre/article/view/45>.
12. Lazaropoulos, A. G., "Smart energy and spectral efficiency (SE) of distribution broadband over power lines (BPL) networks – Part 1: The impact of measurement differences on SE metrics," *Trends in Renewable Energy*, Vol. 4, No. 2, 125-184, Aug. 2018, [Online]. Available: <http://futureenergysp.com/index.php/tre/article/view/76/pdf>.
13. Lazaropoulos, A. G., "Smart energy and spectral efficiency (SE) of distribution broadband over power lines (BPL) networks — Part 2: L1PMA, L2WPMA and L2CXCVC for SE against measurement differences in overhead medium-voltage bpl networks," *Trends in Renewable Energy*, Vol. 4, No. 2, 185-212, Aug. 2018, [Online]. Available: <http://futureenergysp.com/index.php/tre/article/view/77/pdf>.
14. Lazaropoulos, A. G., "Underground distribution BPL connections with (N + 1)-hop repeater systems: A novel capacity mitigation technique," *Elsevier Computers and Electrical Engineering*, Vol. 40, 1813-1826, 2014.
15. Lazaropoulos, A. G., "Review and progress towards the capacity boost of overhead and underground medium-voltage and low-voltage broadband over power lines networks: Cooperative communications through two- and three-hop repeater systems," *ISRN Electronics*, Vol. 2013, Article ID 472190, 1-19, 2013, [Online]. Available: <http://www.hindawi.com/isrn/electronics/aip/472190/>.
16. Lazaropoulos, A. G., "Broadband over power lines (BPL) systems convergence: Multiple-Input Multiple-Output (MIMO) communications analysis of overhead and underground low-voltage and medium-voltage bpl networks (Invited Paper)," *ISRN Power Engineering*, Vol. 2013, Article ID 517940, 1-30, 2013, [Online]. Available: <http://www.hindawi.com/isrn/power.engineering/2013/517940/>.
17. Nazem, A. and M. R. Arshad, "An approach in full duplex digital multipoint systems using large signal power line communication," *Bentham Recent Patents on Electrical & Electronic Engineering*, Vol. 6, No. 2, 138-146, 2013.
18. Lazaropoulos, A. G. and P. G. Cottis, "Transmission characteristics of overhead medium voltage power line communication channels," *IEEE Trans. Power Del.*, Vol. 24, No. 3, 1164-1173, Jul. 2009.
19. Lazaropoulos, A. G. and P. G. Cottis, "Capacity of overhead medium voltage power line communication channels," *IEEE Trans. Power Del.*, Vol. 25, No. 2, 723-733, Apr. 2010.
20. Lazaropoulos, A. G. and P. G. Cottis, "Broadband transmission via underground medium-voltage power lines — Part I: Transmission characteristics," *IEEE Trans. Power Del.*, Vol. 25, No. 4, 2414-2424, Oct. 2010.
21. Lazaropoulos, A. G. and P. G. Cottis, "Broadband transmission via underground medium-voltage power lines — Part II: Capacity," *IEEE Trans. Power Del.*, Vol. 25, No. 4, 2425-2434, Oct. 2010.
22. Lazaropoulos, A. G., "Broadband transmission and statistical performance properties of overhead high-voltage transmission networks," *Hindawi Journal of Computer Networks and Commun.*, 2012, article ID 875632, 2012, [Online]. Available: <http://www.hindawi.com/journals/jncn/aip/875632/>.
23. Biglieri, E., "Coding and modulation for a horrible channel," *IEEE Commun. Mag.*, Vol. 41, No. 5, 92-98, May 2003.
24. Gebhardt, M., F. Weinmann, and K. Dostert, "Physical and regulatory constraints for communication over the power supply grid," *IEEE Commun. Mag.*, Vol. 41, No. 5, 84-90, May 2003.
25. Henry, P. S., "Interference characteristics of broadband power line communication systems using aerial medium voltage wires," *IEEE Commun. Mag.*, Vol. 43, No. 4, 92-98, Apr. 2005.

26. Liu, S. and L. J. Greenstein, "Emission characteristics and interference constraint of overhead medium-voltage broadband power line (BPL) systems," *Proc. IEEE Global Telecommunications Conf.*, 1–5, New Orleans, LA, USA, Nov./Dec. 2008.
27. Götz, M., M. Rapp, and K. Dostert, "Power line channel characteristics and their effect on communication system design," *IEEE Commun. Mag.*, Vol. 42, No. 4, 78–86, Apr. 2004.
28. Lazaropoulos, A. G., "Towards modal integration of overhead and underground low-voltage and medium-voltage power line communication channels in the smart grid landscape: Model expansion, broadband signal transmission characteristics, and statistical performance metrics (Invited Paper)," *ISRN Signal Processing*, Vol. 2012, Article ID 121628, 1–17, 2012, [Online]. Available: <http://www.hindawi.com/isrn/sp/2012/121628/>.
29. Della, D. G. and S. Rinaldi, "Hybrid communication network for the smart grid: Validation of a field test experience," *IEEE Trans. Power Del.*, Vol. 30, No. 6, 2492–2500, 2015.
30. Versolatto, F. and A. M. Tonello, "An MTL theory approach for the simulation of MIMO power-line communication channels," *IEEE Trans. Power Del.*, Vol. 26, No. 3, 1710–1717, Jul. 2011.
31. Amirshahi, P. and M. Kavehrad, "High-frequency characteristics of overhead multiconductor power lines for broadband communications," *IEEE J. Sel. Areas Commun.*, Vol. 24, No. 7, 1292–1303, Jul. 2006.
32. Stadelmeier, L., D. Schneider, D. Schill, A. Schwager, and J. Speidel, "MIMO for inhome power line communications," *Int. Conf. on Source and Channel Coding*, Ulm, Germany, Jan. 2008.
33. Sartenaer, T., "Multiuser communications over frequency selective wired channels and applications to the powerline access network" Ph.D. dissertation, Univ. Catholique Louvain, Louvain-la-Neuve, Belgium, Sep. 2004.
34. Calliacoudas, T. and F. Issa, "Multiconductor transmission lines and cables solver, an efficient simulation tool for plc channel networks development," *IEEE Int. Conf. Power Line Communications and Its Applications*, Athens, Greece, Mar. 2002.
35. Galli, S. and T. Banwell, "A deterministic frequency-domain model for the indoor power line transfer function," *IEEE J. Sel. Areas Commun.*, Vol. 24, No. 7, 1304–1316, Jul. 2006.
36. Galli, S. and T. Banwell, "A novel approach to accurate modeling of the indoor power line channel-Part II: Transfer function and channel properties," *IEEE Trans. Power Del.*, Vol. 20, No. 3, 1869–1878, Jul. 2005.
37. Pérez, A., A. M. Sánchez, J. R. Regué, M. Ribó, R. Aquilué, P. Rodríguez-Cepeda, and F. J. Pajares, "Circuitual and modal characterization of the power-line network in the PLC band," *IEEE Trans. Power Del.*, Vol. 24, No. 3, 1182–1189, Jul. 2009.
38. Sartenaer, T. and P. Delogne, "Deterministic modelling of the (Shielded) outdoor powerline channel based on the multiconductor transmission line equations," *IEEE J. Sel. Areas Commun.*, Vol. 24, No. 7, 1277–1291, Jul. 2006.
39. Sartenaer, T. and P. Delogne, "Powerline cables modelling for broadband communications," *Proc. IEEE Int. Conf. Power Line Communications and Its Applications*, 331–337, Malmö, Sweden, Apr. 2001.
40. Paul, C. R., *Analysis of Multiconductor Transmission Lines*, Wiley, New York, 1994.
41. Faria, J. A. B., *Multiconductor Transmission-Line Structures: Modal Analysis Techniques*, Wiley, New York, 1994.
42. Meng, H., S. Chen, Y. L. Guan, C. L. Law, P. L. So, E. Gunawan, and T. T. Lie, "Modeling of transfer characteristics for the broadband power line communication channel," *IEEE Trans. Power Del.*, Vol. 19, No. 3, 1057–1064, Jul. 2004.
43. Semlyen, A. and B. Gustavsen, "Phase-domain transmission-line modeling with enforcement of symmetry via the propagated characteristic admittance matrix," *IEEE Trans. Power Del.*, Vol. 27, No. 2, 626–631, Apr. 2012.
44. Versolatto, F. and A. M. Tonello, "A MIMO PLC random channel generator and capacity analysis," *Proc. IEEE Int. Symp. Power Line Communications and Its Applications*, 66–71, Udine, Italy, Apr. 2011.

45. Tlich, M., A. Zeddani, F. Moulin, and F. Gauthier, "Indoor power-line communications channel characterization up to 100 MHz — Part I: One-parameter deterministic model," *IEEE Transactions on Power Delivery*, Vol. 23, No. 3, 1392–1401, 2008.
46. Tonello, A. M. and T. Zheng, "Bottom-up transfer function generator for broadband PLC statistical channel modeling," *Proc. IEEE International Symposium on Power Line Communications and Its Applications 2009, ISPLC 2009*, 7–12, Mar. 2009.
47. Tonello, A. M. and F. Versolatto, "Bottom-up statistical PLC channel modeling — Part I: Random topology model and efficient transfer function computation," *IEEE Transactions on Power Delivery*, Vol. 26, No. 2, 891–898, 2011.
48. Pittolo, A. and A. M. Tonello, "A synthetic statistical mimo plc channel model applied to an in-home scenario," *IEEE Transactions on Communications*, Vol. 65, No. 6, 2543–2553, 2017.
49. Tonello, A. M. and F. Versolatto, "Bottom-up statistical PLC channel modeling — Part II: Inferring the statistics," *IEEE transactions on Power Delivery*, Vol. 25, No. 4, 2356–2363, 2010.
50. Sancha, S., F. J. Canete, L. Diez, and J. T. Entrambasaguas, "A channel simulator for indoor power-line communications," *Proc. IEEE International Symposium on Power Line Communications and Its Applications 2007. ISPLC'07*, 104–109, Mar. 2007.
51. Heathcote, A., S. Brown, and D. Cousineau, "QMPE: Estimating lognormal, Wald, and Weibull RT distributions with a parameter-dependent lower bound," *Behavior Research Methods, Instruments, & Computers*, Vol. 36, No. 2, 277–290, 2004.
52. Lazaropoulos, A. G., "Statistical broadband over power lines (BPL) channel modeling — Part 2: The numerical results of the statistical hybrid model," *Progress In Electromagnetics Research B*, under review.
53. "OPERA1, D5: Pathloss as a function of frequency, distance and network topology for various LV and MV European powerline networks," IST Integrated Project No. 507667, Apr. 2005.
54. Van der Wielen, P. C. J. M., "On-line detection and location of partial discharges in medium-voltage power cables" Ph.D. dissertation, Tech. Univ. Eindhoven, Eindhoven, the Netherlands, Apr. 2005.
55. Van der Wielen, P. C. J. M., E. F. Steennis, and P. A. A. F. Wouters, "Fundamental aspects of excitation and propagation of on-line partial discharge signals in three-phase medium voltage cable systems," *IEEE Trans. Dielectr. Electr. Insul.*, Vol. 10, No. 4, 678–688, Aug. 2003.
56. Amirshahi, P., "Broadband access and home networking through powerline networks" Ph.D. dissertation, Pennsylvania State Univ., University Park, PA, May 2006.
57. M. D'Amore and M. S. Sarto, "A new formulation of lossy ground return parameters for transient analysis of multiconductor dissipative lines," *IEEE Trans. Power Del.*, Vol. 12, No. 1, 303–314, Jan. 1997.
58. Amirshahi, P. and M. Kavehrad, "Medium voltage overhead powerline broadband communications; Transmission capacity and electromagnetic interference," *Proc. IEEE Int. Symp. Power Line Commun. Appl.*, 2–6, Vancouver, BC, Canada, Apr. 2005.
59. D'Amore, M. and M. S. Sarto, "Simulation models of a dissipative transmission line above a lossy ground for a wide-frequency range — Part I: Single conductor configuration," *IEEE Trans. Electromagn. Compat.*, Vol. 38, No. 2, 127–138, May 1996.
60. D'Amore, M. and M. S. Sarto, "Simulation models of a dissipative transmission line above a lossy ground for a wide-frequency range — Part II: Multi-conductor configuration," *IEEE Trans. Electromagn. Compat.*, Vol. 38, No. 2, 139–149, May 1996.
61. Suljanović, N., A. Mujčić, M. Zajc, and J. F. Tasič, "Approximate computation of high-frequency characteristics for power line with horizontal disposition and middle-phase to ground coupling," *Elsevier Electr. Power Syst. Res.*, Vol. 69, 17–24, Jan. 2004.
62. Suljanović, N., A. Mujčić, M. Zajc, and J. F. Tasič, "High-frequency characteristics of high-voltage power line," *Proc. IEEE Int. Conf. on Computer as a Tool*, 310–314, Ljubljana, Slovenia, Sep. 2003.
63. Suljanović, N., A. Mujčić, M. Zajc, and J. F. Tasič, "Power-line high-frequency characteristics: analytical formulation," *Proc. Joint 1st Workshop on Mobile Future & Symposium on Trends in*

- Communications*, 106–109, Bratislava, Slovakia, Oct. 2003.
64. Villiers, W., J. H. Cloete, and R. Herman, “The feasibility of ampacity control on HV transmission lines using the PLC system,” *Proc. IEEE Conf. Africon*, Vol. 2, 865–870, George, South Africa, Oct. 2002.
  65. “OPERA1, D44: Report presenting the architecture of plc system, the electricity network topologies, the operating modes and the equipment over which PLC access system will be installed,” IST Integr. Project No. 507667, Dec. 2005.
  66. Anatory, J., N. Theethayi, R. Thottappillil, M. M. Kissaka, and N. H. Mvungi, “The influence of load impedance, line length, and branches on underground cable Power-Line Communications (PLC) systems,” *IEEE Trans. Power Del.*, Vol. 23, No. 1, 180–187, Jan. 2008.
  67. Anatory, J., N. Theethayi, and R. Thottappillil, “Power-line communication channel model for interconnected networks — Part II: Multiconductor system,” *IEEE Trans. Power Del.*, Vol. 24, No. 1, 124–128, Jan. 2009.
  68. Anatory, J., N. Theethayi, R. Thottappillil, M. M. Kissaka, and N. H. Mvungi, “The effects of load impedance, line length, and branches in typical low-voltage channels of the BPLC systems of developing countries: transmission-line analyses,” *IEEE Trans. Power Del.*, Vol. 24, No. 2, 621–629, Apr. 2009.
  69. Banwell, T. and S. Galli, “A novel approach to accurate modeling of the indoor power line channel — Part I: Circuit analysis and companion model,” *IEEE Trans. Power Del.*, Vol. 20, No. 2, 655–663, Apr. 2005.
  70. Villiers, W., J. H. Cloete, L. M. Wedepohl, and A. Burger, “Real-time sag monitoring system for high-voltage overhead transmission lines based on power-line carrier signal behavior,” *IEEE Trans. Power Del.*, Vol. 23, No. 1, 389–395, Jan. 2008.
  71. Lazaropoulos, A. G., “New coupling schemes for distribution broadband over power lines (BPL) networks,” *Progress In Electromagnetics Research B*, Vol. 71, 39–54, 2016.
  72. NTIA, “Potential interference from broadband over power line (BPL) systems to federal government radio communications at 1.7–80 MHz — Phase 1 Study, Vol. 1,” NTIA Rep. 04-413, Apr. 2004.
  73. NATO, “HF Interference, Procedures and Tools (Interférences HF, procédures et outils) Final Report of NATO RTO Information Systems Technology,” RTO-TR-ISTR-050, Jun. 2007.
  74. Lazaropoulos, A. G., “The impact of noise models on capacity performance of distribution broadband over power lines networks,” *Hindawi Computer Networks and Communications*, Vol. 2016, Article ID 5680850, 14 pages, 2016, doi:10.1155/2016/5680850, [Online]. Available: <http://www.hindawi.com/journals/jcnc/2016/5680850/>.
  75. Lazaropoulos, A. G., “Detection of energy theft in overhead low-voltage power grids — The hook style energy theft in the smart grid era,” *Trends in Renewable Energy*, Vol. 5, No. 1, 12-46, Oct. 2018, [Online]. Available: <http://futureenergysp.com/index.php/tre/article/view/81/pdf>.
  76. <http://matlabtricks.com/post-44/generate-random-numbers-with-a-given-distribution>.
  77. <http://www.av8n.com/physics/arbitrary-probability.htm>.
  78. Chhikara, R., *The Inverse Gaussian Distribution: Theory, Methodology, and Applications*, Vol. 95, CRC Press, 1988.
  79. Koizumi, D., “On the maximum likelihood estimation of Weibull distribution with lifetime data of hard disk drives,” *Proc. Int’l Conf. Par. and Dist. Proc. Tech. and Appl., PDPTA’17*, 314–320, 2017.
  80. Nwobi, F. N. and C. A. Ugomma, “A comparison of methods for the estimation of Weibull distribution parameters,” *Metodoloski Zvezki*, Vol. 11, No. 1, 65–78, 2015.
  81. Mahdi, S. and M. Cenac, “Estimating parameters of gumbel distribution using the methods of moments, probability weighted moments and maximum likelihood,” *Revista de Matemática: Teoría y Aplicaciones*, Vol. 12, No. 1–2, 151–156, 2005.